Journal of Power Sources 196 (2011) 4859–4864

Contents lists available at ScienceDirect

Journal of Power Sources

journal homepage: www.elsevier.com/locate/jpowsour

Electrophoretic deposition of ZnO film and its compression for a plastic based flexible dye-sensitized solar cell

Hsin-Wei Chen[a], Chia-Yu Lin[a], Yi-Hsuan Lai[a], Jian-Ging Chen[a], Chun-Chieh Wang[a], Chih-Wei Hu[b], Chih-Yu Hsu[a], R. Vittal[a], Kuo-Chuan Ho[a,b,*]

[a] Department of Chemical Engineering, National Taiwan University, Taipei 10617, Taiwan
[b] Institute of Polymer Science and Engineering, National Taiwan University, Taipei 10617, Taiwan

ARTICLE INFO

Article history:
Received 23 October 2010
Received in revised form
29 December 2010
Accepted 20 January 2011
Available online 26 January 2011

Keywords:
Compression method
Electrophoretic deposition
Flexible dye-sensitized solar cell
Room temperature fabrication method
UV–O_3-treatment

ABSTRACT

A room temperature fabrication method is developed for the preparation of a ZnO porous film on a plastic substrate, involving an electrophoresis deposition (EPD) process, followed by the compression of the film as the post-treatment. The thus prepared ZnO film is used for the photoanode of a dye-sensitized solar cell (DSSC). Besides, an indoline dye is employed as the sensitizer (referred to as D149) for the ZnO semiconductor. Performances of such DSSCs are studied at various compression pressures used for their ZnO films. Electrochemical impedance spectroscopy (EIS) is employed to quantify the charge transport resistance at the ZnO/dye/electrolyte interface (R_{ct2}) and the electron lifetime (τ_e) in the ZnO film. As for the thickness effect, ZnO film with a thickness of about 22 μm renders the best efficiency for the ZnO based DSSC. In addition, UV–O_3 is applied in two ways; in one way only the compressed ZnO film is treated in one step, and in the second way both the substrate and the compressed ZnO film are treated separately in two steps. The adherence of the ZnO film is shown by a photograph. Scanning electron microscopy is used to characterize the morphologies of the ZnO films.

1. Introduction

Flexible dye-sensitized solar cells (DSSCs) have attracted much attention, because they are handy and are convenient for transportation. In particular, flexible DSSCs using thin and lightweight conducting plastic substrates for their photoelectrodes are cheap and they are suitable for roll-to-roll production [1,2]. ZnO has been investigated as a promising alternative photoanode material for DSSCs since the inception of research on TiO_2-based DSSCs, due to its high electronic mobility and due to the fact that both ZnO and TiO_2 have almost the same band gap energies, i.e., ~3.2 eV and ~3.3 eV, respectively [3–9]. Several techniques, e.g., chemical bath deposition [6], screen printing [5], drop cast [9], doctor blading [3], electrospinning [7], electro-deposition [10] and electrophoretic deposition (EPD) [11] have been developed to prepare ZnO electrodes. However, most of these conventional methods involve high-temperature sintering at 450–500 °C for annealing the ZnO nanoparticles, in order to obtain good connection among the particles; this high temperature cannot be used in the case of plastic substrates. Therefore, it is necessary, in the case of plastic substrates, to develop a new fabrication method accomplishable below 150 °C, with some post-treatment, if necessary, to enhance the connection among the ZnO particles. Some such methods applied in the case of TiO_2 based DSSCs [2,12–17] can be utilized in the case of ZnO based DSSCs. Among these methods, we selected for this research a low-temperature method for preparing the ZnO film involving its compression process as the post-treatment; this selection was based on previous reports on such methods, which were however used in the case of TiO_2 films [18–20]. There have been a few reports on the fabrication of ZnO based DSSCs with plastic substrates [8,10,11,21]. However, there is no report on the employment of a low temperature post-treatment process for the preparation of a ZnO-photoanode.

In this study, we used compression and UV–O_3-treatment as the post-treatments for ZnO particles deposited by electrophoresis, intending to enhance the connectivity among the particles. This compression method is quite simple and rapid in nature to prepare a ZnO-photoelectrode for a plastic based flexible DSSC. The fabrication of the pertinent photoelectrode is free of sintering or annealing process and is accomplished at the room temperature, except for the dye adsorption. In addition, we also studied the compression effect using electrochemical impedance spectroscopy (EIS), and examined the morphologies of the as-deposited film and compressed film through scanning electron microscopy (SEM). In

* Corresponding author at: Department of Chemical Engineering, National Taiwan University, No. 1, Sec. 4, Roosevelt Rd., Taipei 10617, Taiwan. Tel.: +886 2 2366 0739; fax: +886 2 2362 3040.
E-mail address: kcho@ntu.edu.tw (K.-C. Ho).

0378-7753/$ – see front matter © 2011 Elsevier B.V. All rights reserved.
doi:10.1016/j.jpowsour.2011.01.057

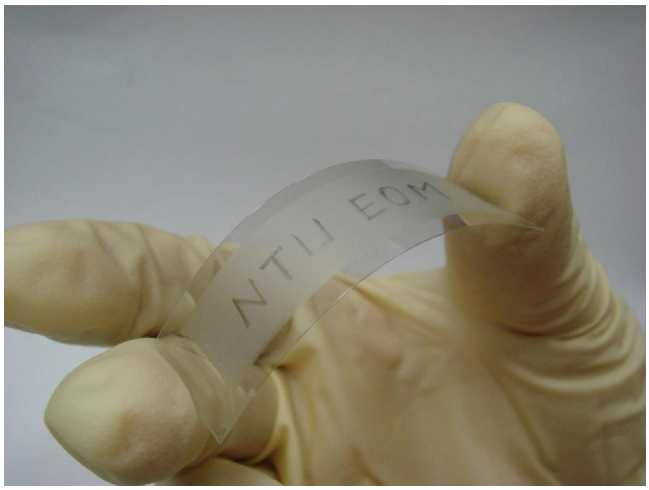

Fig. 1. Photograph of a bent ZnO film compressed at 100 MPa on ITO–PEN substrate; the image has writings with a HB pencil.

order to improve the light-to-electricity conversion efficiency of the flexible DSSC, we adjusted the compression pressure, thickness of the ZnO film, treated the ZnO film with UV–O_3 (for photocatalytic decomposition of organic residues), and activated the ITO–PEN substrate through UV–O_3 treatment. We have achieved a conversion efficiency (η) of 4.04% for a ZnO-based flexible DSSC fabricated at low temperature.

This is the first time that compression post-treatment is used on the ZnO film on a plastic conducting substrate to improve the conversion efficiency of the pertinent DSSC. Besides, expensive ruthenium dye is avoided in this study and a metal-free organic indoline dye is used, which rendered efficiency for its DSSC, comparable to that of a cell with a plastic substrate and a ruthenium dye. The dye has an extinction coefficient of 68,700 mol^{-1} cm^{-1} at 526 nm, which is five times higher than that of the conventional Ru dye, N719 (13,900 mol^{-1} cm^{-1} at 541 nm).

2. Experimental

2.1. Materials

Lithium iodide (LiI) and iodine (I_2) were obtained from Merck; acetonitrile (ACN) and tertiary butanol were also obtained from Merck and their water molecules were removed by molecular sieves (4 Å). Tert-butyl alcohol was obtained from Acros; ethanol and isopropyl alcohol (IPA) were obtained from Aldrich. ZnO powders (20 nm) were obtained from Uni-Onward (Taipei, Taiwan). FTO glass (15 Ω $sq.^{-1}$) and 1,2-dimethyl-3-propylimidazolium iodide (DMPII) were obtained from Solaronix S.A., Aubonne, Switzerland. ITO–PEN (15 Ω $sq.^{-1}$, Peccell Technologies Inc.) was used as the substrate for the ZnO photoanode.

2.2. Preparation of ZnO suspension and the corresponding photoanode

Commercial nanocrystalline ZnO powder (20 nm) was dispersed well in isopropyl alcohol (IPA) at 6 g L^{-1}, without using any surfactant or additive. The suspension was stirred for at least 3 h and then ultrasonicated for 20 min. After ultrasonication the ZnO suspension was put in a container for electrophoresis; an FTO glass was used as the anode and the conducting plastic substrate as the cathode during the EPD process. The EPD was performed at a DC electric field of 200 V cm^{-1} for 1 min; longer deposition time was used to increase the film thickness. After finishing the EPD process, the residual IPA solvent on the as-deposited film was evaporated for a

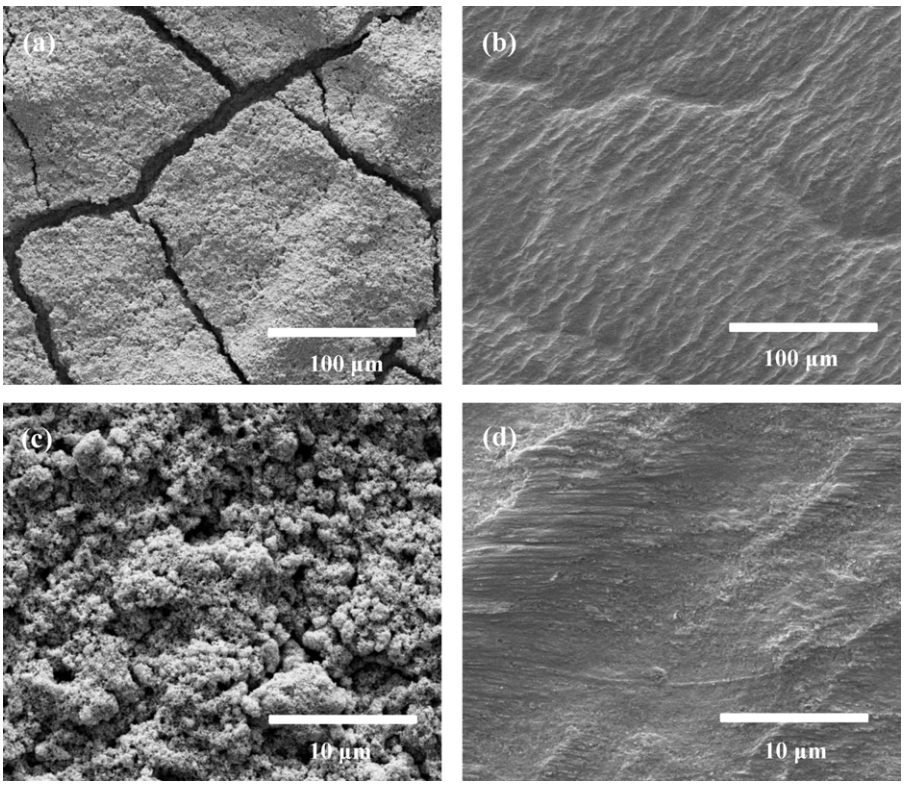

Fig. 2. Top views of SEM micrographs of the electrophoretically deposited ZnO film on the ITO–PEN substrate: (a) as deposited film (low magnification, 100 μm), (b) the film after mechanical compression (low magnification, 100 μm), (c) as deposited film (high magnification, 10 μm), and (d) the film after mechanical compression (high magnification, 10 μm).

few seconds in air at ambient temperature. As the post-treatment of the nanostructured ZnO film obtained by the EPD process, mechanical compression (MTS-810, Material Testing System, Eden Prairie, MN, USA) was applied at different pressures (25–100 MPa). The ZnO electrodes were immersed at 50 °C for 3 h in a 0.5 mM solution of D149 (Mitsubishi Co.) in acetonitrile and tert-butyl alcohol (volume ratio of 1:1), containing also 1 mM of chenodeoxycholic acid (CDCA) as the co-adsorbant. The ZnO electrode prepared as described above was coupled with a platinum counter electrode (PE-CE), made of ITO glass with Pt, Pt being sputtered for 120 s. The electrodes were separated by a 25 μm-thick Surlyn tape (SX1170-25, Solaronix S.A., Aubonne, Switzerland) and sealed by heating. A mixture of 0.1 M LiI, 0.05 M I_2, 0.6 M DMPII in acetonitrile was used as the electrolyte. The electrolyte was injected into the gap between the two electrodes by capillarity; the electrolyte-injecting hole was previously made in the counter electrode with a drilling machine, and the hole was sealed with hot-melt glue after the injection of the electrolyte. The size (area) of the ZnO photoanode was first adjusted by a cotton swap rinsed with ethanol to scrap the ZnO thin film, so as to control the photoanode with a specific area (1.0 cm by 1.0 cm), followed by confining it with a mask (0.55 cm in diameter).

2.3. Instrumentation

The surface of the DSSC was illuminated by a class A quality solar simulator (PEC-L11, AM1.5G, Peccell Technologies Inc.) and an incident light intensity of 100 mW cm^{-2} was calibrated with a standard Si cell (PECSI01, Peccell Technologies Inc.). The photoelectrochemical characteristics and electrochemical impedance spectra (EIS) of the cells were recorded using a potentiostat/galvanostat (PGSTAT 30, Autolab, Eco-Chemie, the Netherlands) under 100 mW cm^{-2} light intensity. The frequency range explored for impedance measurements was 10 mHz to 65 kHz. The applied bias voltage was set at the open-circuit voltage of the DSSC, between the ITO–Pt–CE and the PEN–ZnO–dye working electrode, starting from the short-circuit condition; the corresponding AC amplitude was 10 mV. The impedance spectra were analyzed using a completely new equivalent circuit model. The film thickness was determined using a surface profilometer (Sloan Dektak 3030). Morphologies of the films were observed by scanning electron microscopy (SEM, Nova NanoSEM 230, FEI Ultra-High Resolution FE-SEM with low vacuum mode).

3. Results and discussion

3.1. The ZnO film and its compression-post-treatment

In this study, the distance between the electrodes, and the ZnO concentration in the EPD solution were kept unchanged. We observed that light could be scattered well by the as-deposited film obtained through the EPD process. The film could be easily damaged by scratching, because of its poor intrinsic mechanical strength; however, its adhesion on the plastic substrate was excellent, as observed from the fact that the film after its compression could not be peeled off from the substrate even after bending the substrate. The great adherence of the film to the substrate can be attributed to the highly ordered structure of the particles with a large packing density and capillary stress. As for the adhesion test, we used a HB pencil to write on the compressed (100 MPa) ZnO photoanode and bent the film as shown in Fig. 1. It is clear from the figure that the ZnO film remains intact even at a great bending angle. Fig. 2 shows top view SEM images of an as-deposited ZnO film at different magnifications, deposited under a DC electric field of 200 V cm^{-1}. As can be seen in Fig. 2a, the as-deposited film is full of microcracks and the film seems to be very rough and porous. It was already mentioned that the adherence of the film to the substrate was excellent and the film could be handled well without exfoliation. It is quite important that a nanostructured ceramic film is homogeneous and has no or fewer cracks; for this reason, a compression is applied to the film as its post-treatment process intending to diminish the microcracks in the film and to make it smooth. Fig. 2b shows the SEM image of compressed version (100 MPa) of the film shown in Fig. 2a, magnification being the same in both the cases. We can observe in Fig. 2b that the morphology of the film is significantly altered after the employment of the mechanical compression. The compressed film is homogeneous and smooth, with reference to the as-deposited film. Besides, the cracks of the film are totally reduced and the film is smoothened after the mechanical compression. Fig. 2c shows the as-deposited film at a different magnification and Fig. 2d shows its compressed version at the same magnification. The compression-post-treatment is employed to enable better inter-particle connection of ZnO particles and to homogenize the film surface. Besides, such compressed films are transparent and scatter light to a lesser extent than the as-deposited film.

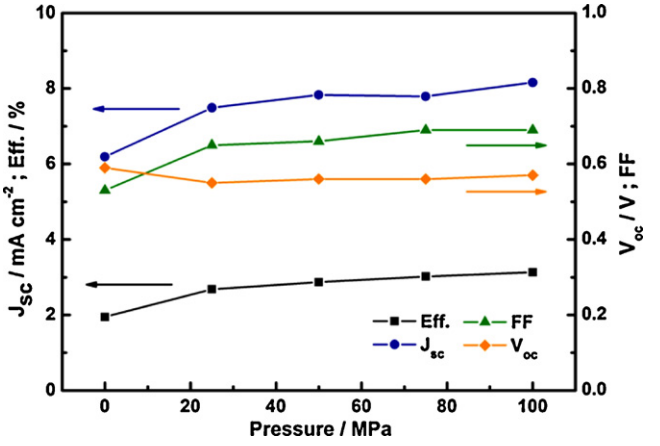

Fig. 3. Variation of photovoltaic parameters, i.e., short-circuit photocurrent (J_{sc}), open-circuit voltage (V_{oc}), fill factor (FF), and light-to-electricity conversion efficiency (η) of ZnO-based DSSCs, depending on the compression pressure used for their ZnO films (thickness of each film: 20 μm).

3.2. Relationship between the compression pressure and the light-to-electricity conversion efficiency

Fig. 3 illustrates the variation of photovoltaic parameters, i.e., short-circuit photocurrent density (J_{sc}), open-circuit voltage (V_{oc}), fill factor (FF), and light-to-electricity conversion efficiency (η) of ZnO-based DSSCs, depending on the compression-pressure used for their ZnO films (thickness of each film: 20 μm); Table 1 summarizes the corresponding parameters. Table 1 shows that the fill factors (FFs) are all high, especially with compression; these high fill factors indicate strong contacts between the films and their substrates. Besides, the FF increases with increase in the compression pressure. The open-circuit voltage (V_{oc}) does not change much with compression pressure. Interestingly, it can be seen that the

Table 1
Photovoltaic parameters of the DSSCs at different compression pressures for their ZnO films (film thickness: 20 μm).

Pressure (MPa)	V_{oc} (V)	J_{sc} (mA cm^{-2})	FF	Efficiency (%)
None	0.59	6.19	0.53	1.95
25	0.55	7.49	0.65	2.68
50	0.56	7.83	0.66	2.87
75	0.56	7.79	0.69	3.02
100	0.57	8.16	0.69	3.13

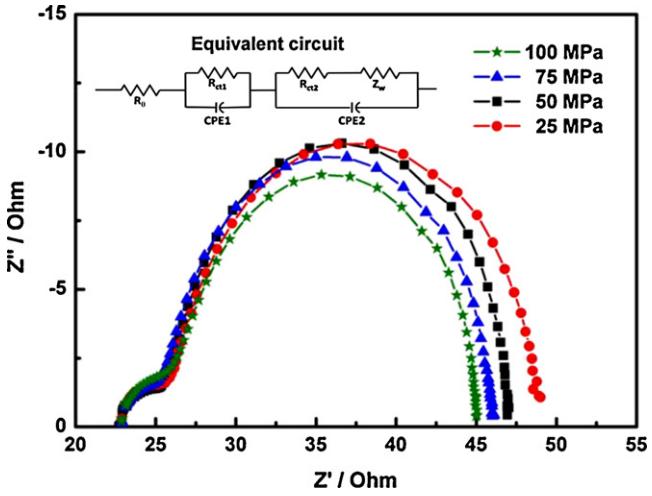

Fig. 4. Electrochemical impedance spectra of the DSSCs, at different compression pressures for their ZnO films (film thickness: 20 μm). The equivalent circuit of this study is shown in the inset.

short-circuit photocurrent density density (J_{sc}) and the light-to-electricity conversion efficiency (η) have direct relationship to the compression pressure (Fig. 3), i.e., they both show increases with the increase of compression pressure. The improvement in J_{sc} with higher compression (Fig. 3) is due to the associated higher coordination number (N) and better inter-particle connections, which enable longer electron lifetime and higher electron diffusion coefficient. The coordination number (N) could be calculated by the following equation [22]:

$$N = \frac{3.08}{P_P} - 1.13 \quad (1)$$

where P_p is the porosity of the pressed film. It is logical to think that the porosity of the film decreases with the increase of compression pressure; this can also be seen in Fig. 2 where the film becomes smooth with compression, i.e., without cracks or pores. After compression post-treatment, the thickness of ZnO film decreases to about 65% of the as-deposited EPD film. According to the above equation, the coordination number (N) increases with the decrease in porosity, which means that the connectivity between the particles increases with the decrease of porosity, that is with the increase of compression. Thus the increased coordination number (N) or better inter-particle connections enabled higher J_{sc} for the DSSCs with compressed ZnO films. From the point of view of electron transport, N of 5 implies an electron residing on a particular particle with 5 possible directions in which it can move to an adjacent particle.

Furthermore, electrochemical impedance spectroscopy (EIS) was used to study the internal resistances and the charge transfer kinetics of the mesoporous ZnO films in the DSSCs. Fig. 4 shows Nyquist plots of the DSSCs (under 100 mW cm^{-2}) with ZnO films of same thickness (~20 μm), compressed at different pressures. The impedance spectra are interpreted and modeled using the equivalent circuit proposed in the inset of Fig. 4. The Nyquist plots essentially consist of two sets of semicircles. The smaller semicircle at higher frequencies (kHz range) corresponds to the charge-transfer resistances at the counter electrode/electrolyte interface (R_{ct1}) and at the electrical contacts between conductive substrate/ZnO or among ZnO particles. The larger circle at lower frequencies (10–100 Hz range) represents the resistances against electron transfer in the ZnO layer and charge-transfer process at the ZnO/dye/electrolyte interface (R_{ct2}), and against ion diffusion within the electrolyte (R_{diff}). R_{diff} is virtually overlapped by R_{ct2} due to relatively short length for I^- ion diffusion caused by the thin spacer (25 μm thick) used by us. Identical semicircles at high frequency region indicate, as expected, that the ZnO-based photoanodes with different compressions do not affect the charge transfer process at the counter electrode/electrolyte interface of their DSSCs. Table 2 shows the corresponding values of R_{ct1} and R_{ct2}. It can be seen in the table that the value of R_{ct2} decreases as the compressed pressure increases from 25 to 100 MPa; this trend can also be clearly seen in Fig. 4. This phenomenon is related to the increase in the coordination number (N), which enables better interconnectivity among the ZnO particles and stronger adherence of the particles to the ITO–PEN substrate; decreased pore sizes due to increased compression enhances the inter-particles connection among the ZnO particles, which in turn decreases the charge transfer resistance, R_{ct2}. In Fig. 4 and Table 2, it can be seen that the mesoporous ZnO film, compressed at 100 MPa has least values of R_{ct1} and R_{ct2}.

Table 2
Electrochemical impedance spectra (EIS) parameters of the DSSCs, at different compression pressures for their ZnO films (film thickness: 20 μm).

Pressure (MPa)	R_{ct1} (Ω)	R_{ct2} (Ω)	f_{max} (s^{-1})	τ_e (ms)
25	4.20	24.03	76.3	2.09
50	4.11	22.32	75.7	2.10
75	4.02	20.95	62.3	2.55
100	3.89	19.71	51.1	3.11

In addition, electron lifetimes (τ_e) in the ZnO films of same thickness (~20 μm), obtained at different pressures were determined using Bode-phase plots (Fig. 5). The Bode phase plots of EIS spectra, as shown in Fig. 5, display the frequency peaks of the charge transfer process at different interfaces of the cells, with ZnO-films compressed at different pressures. The characteristic low frequency peaks (f_{max}) are located as shown in Table 2. The characteristic frequency peaks show a shift toward lower frequencies with the increase of compression pressure; this means a longer electron lifetime is obtained when the compression pressure is increased from 25 to 100 MPa. The calculated electron lifetimes are also shown in Table 2. These observations imply that an increase in the compression pressure for the ZnO film increases the connection among ZnO particles, which in turn decreases the electron transfer resistance and thereby increases the electron lifetime in the ZnO film.

3.3. *Effects of thickness of a ZnO film and UV–O_3 treatment for the film on the photovoltaic performance of a DSSC*

Table 3 shows the photovoltaic parameters of DSSCs with ZnO films of different thickness, each film compressed at the pressure

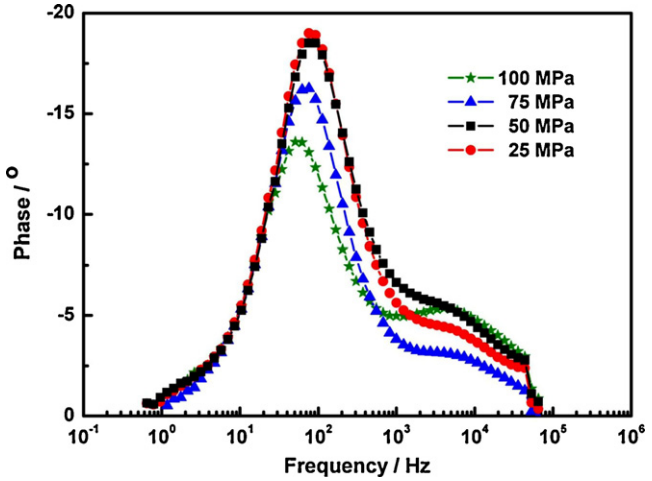

Fig. 5. Bode phase plots of the DSSCs, at different compression pressures for their ZnO films (film thickness: 20 μm).

Table 3
Photovoltaic parameters of the DSSCs with ZnO films of different thickness, each film being compressed at 100 MPa.

Thickness (μm)	V_{oc} (V)	J_{sc} (mA cm^{-2})	FF	Efficiency (%)
10	0.57	6.69	0.60	2.31
14	0.56	6.86	0.63	2.42
18	0.56	7.02	0.64	2.51
22	0.58	8.16	0.70	3.36
26	0.57	8.04	0.68	3.11

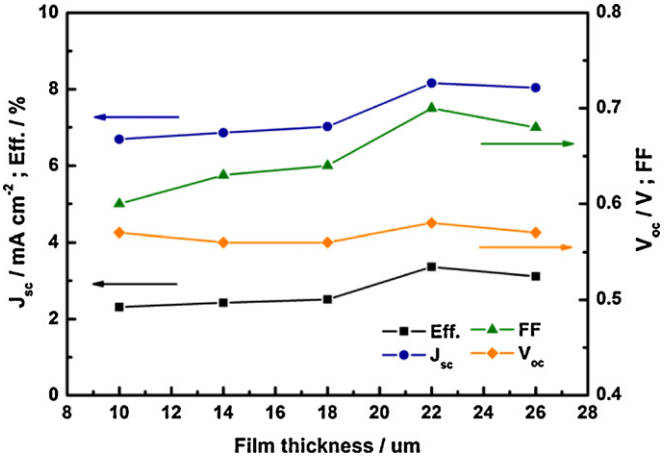

Fig. 6. Variation of photovoltaic parameters, i.e., short-circuit photocurrent (J_{sc}), open-circuit voltage (V_{oc}), fill factor (FF), and light-to-electricity conversion efficiency (η) of ZnO-based DSSCs, depending on the thickness of their ZnO films, each film being compressed at 100 MPa.

of 100 MPa. Fig. 6 illustrates the variation of photovoltaic parameters, i.e., J_{sc}, V_{oc}, FF, and η of ZnO-based DSSCs, depending on the thickness of their ZnO films, each film being compressed at 100 MPa. It can be seen in Fig. 6 that the mesoporous ZnO film with a thickness of about 22 μm renders the best cell efficiency of 3.36% for its DSSC. Fig. 7a and b shows at different magnifica-

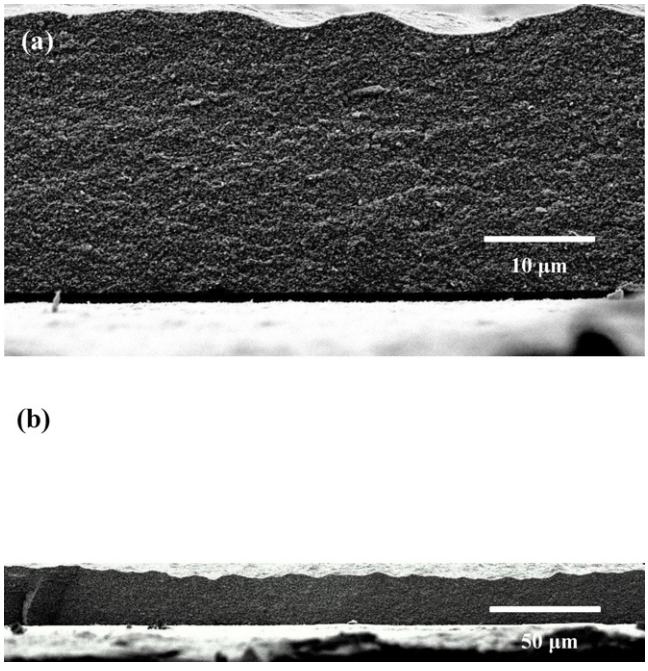

Fig. 7. Cross-sectional SEM images of an electrophoretically deposited ZnO film (thickness: about 26 μm) at different magnifications; the film was compressed at 100 MPa.

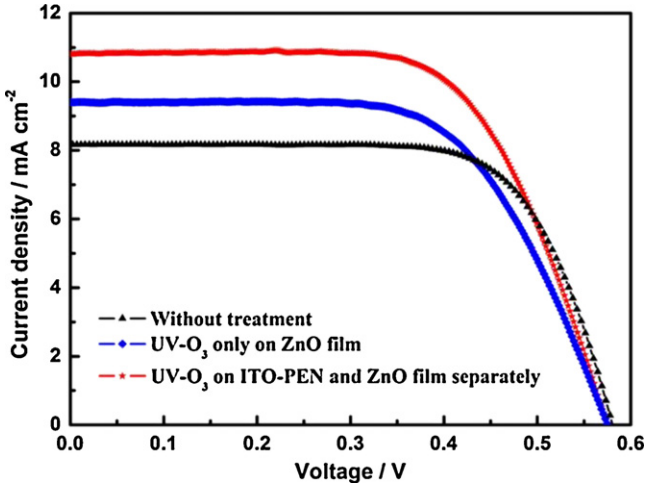

Fig. 8. Photocurrent–voltage curves of DSSCs with ZnO films of 22 μm thickness when the UV–O_3 treatment was applied in one case to only ZnO film (single step) and in the other case to the ITO–PEN and its ZnO film separately (double step).

tions the SEM cross-sectional images of the ZnO film (thickness: about 26 μm), compressed at 100 MPa; both figures show that the film is quite homogeneous and its structure is very compact after the compression post-treatment. If the film thickness is increased beyond 22 μm, all the photovoltaic parameters, i.e, V_{oc}, J_{sc}, FF and η show a decrease (Table 3). Increased thickness of a semiconductor film in a DSSC hinders electron transfer in the film, because electron lifetime is insufficient in such cases and the electrons tend to combine with I_3^- ions and thereby decrease the J_{sc} and V_{oc}, which consequently reduces the FF and η of the cell.

It was speculated that UV–O_3 treatment could be used to decompose some organic residues or impurities. Some organic residues were expected to present in the mesoporous ZnO film prepared by electrophoretic deposition. UV–O_3 was applied in two ways; in one way only the compressed ZnO film was treated in one step, and in the second way both the substrate and the compressed ZnO film were treated separately in two steps. An apparent improvement can be seen in the J_{sc} after the UV–O_3 treatment of the ZnO film (Fig. 8). This improvement is attributed to the photocatalytic decomposition and removal of organic residues and some contaminant impurities in the film by the UV light irradiation in the presence of O_3. Usually researchers use deionized water (DIW) and ethanol to clean the substrate. We observed that the wettability of an ITO–PEN substrate is poor and the surface is hydrophobic. Besides, there may be some organic contamination or impurity on the ITO–PEN surface. Therefore, we performed surface activation for the ITO–PEN film by means of the UV–O_3 treatment, and did the treatment once again for the whole photoanode with the ZnO film. The UV–O_3 treatment was

Table 4
Influence of UV–O_3 treatment (15 min) applied in one case to only ZnO film (single step) and in the other case to the ITO–PEN and its ZnO film separately (double step) on the performance of the DSSCs.

UV–O_3 treatment	V_{oc} (V)	J_{sc} (mA cm^{-2})	FF	Efficiency (%)
Without treatment	0.58	8.16	0.70	3.36
Only on ZnO film	0.58	9.39	0.63	3.42
On ITO–PEN and ZnO film separately	0.57	10.82	0.65	4.04

expected to decompose the organic residues adsorbed on the surface of the ITO–PEN. After the UV–O_3 treatment, we could see the suppression of the contact angle of water droplet placed on the ITO–PEN surface; this implies that the hydrophilicity of the surface is increased. This increased hydrophilicity has probably enhanced the adhesion of the ZnO film to the substrate. This indeed is vindicated by the increases in the J_{sc} and other photovoltaic parameters of the DSSC with UV–O_3 treatment for both the substrate and the photoanode; these increases can be seen in Table 4.

4. Conclusions

Nanostructured ZnO films were deposited on ITO–PEN substrate by an electrophoresis deposition (EPD) method, and the films were subjected to post-treatment by mechanical compression. The compressed film is homogeneous and smooth, with reference to the as-deposited film (Figs. 2b and d and 7). Besides, cracks of the film are totally reduced (Fig. 2b and d). The photocurrent density (J_{sc}) and the light-to-electricity conversion efficiency (η) of a cell with the ZnO film have direct relationship to the compression pressure applied to the film, i.e., they both show increase with the increase of compression pressure (Fig. 3 and Table 1). Electrochemical impedance spectra (EIS, Fig. 4) show that the R_{ct2} value of a DSSC decreases as the compression pressure increases from 25 MPa to 100 MPa (Table 2). The ZnO film subjected to highest compression pressure of 100 MPa enables the longest electron lifetime (τ_e) in the film for its DSSC (Fig. 5 and Table 2). The mesoporous ZnO film with a thickness of about 22 μm renders the best cell efficiency of 3.36% for its DSSC (Table 3). SEM cross-sectional images of the ZnO film show that the film is quite homogeneous and its structure is very compact after the compression post-treatment (Fig. 7). Increase of thickness of a ZnO film beyond 22 μm (with compression) results in a decrease of efficiency for its DSSC. UV–O_3 treatment of the ZnO film enables a slightly increased efficiency (3.42%) for its cell, compared to that of the cell without such treatment (3.36%); such treatment for the ITO–PEN substrate and again for the whole photoanode with the ZnO film gives much more higher conversion efficiency (4.04%) for the pertinent cell.

Acknowledgements

This work was financially sponsored by a grant from the National Taiwan University. Some of the instruments used in this study were made available through the support of the National Science Council (NSC) of Taiwan.

References

[1] M. Gratzel, Nature 414 (2001) 338–344.
[2] T. Yamaguchi, N. Tobe, D. Matsumoto, T. Nagai, H. Arakawa, Solar Energy Materials and Solar Cells 94 (2010) 812–816.
[3] M. Saito, S. Fujihara, Energy and Environmental Science 1 (2008) 280–283.
[4] H.Q. Liu, G. Piret, B. Sieber, J. Laureyns, P. Roussel, W.G. Xu, R. Boukherroub, S. Szunerits, Electrochemistry Communications 11 (2009) 945–949.
[5] W. Chen, H.F. Zhang, I.M. Hsing, S.H. Yang, Electrochemistry Communications 11 (2009) 1057–1060.
[6] E. Hosono, Y. Mitsui, H.S. Zhou, Dalton Transactions (2008) 5439–5441.
[7] W. Zhang, R. Zhu, X.Z. Liu, B. Liu, S. Ramakrishna, Applied Physics Letters 95 (2009).
[8] C.Y. Jiang, X.W. Sun, K.W. Tan, G.Q. Lo, A.K.K. Kyaw, D.L. Kwong, Applied Physics Letters 92 (2008).
[9] Q.F. Zhang, T.R. Chou, B. Russo, S.A. Jenekhe, G.Z. Cao, Angewandte Chemie-International Edition 47 (2008) 2402–2406.
[10] T. Yoshida, J.B. Zhang, D. Komatsu, S. Sawatani, H. Minoura, T. Pauporte, D. Lincot, T. Oekermann, D. Schlettwein, H. Tada, D. Wohrle, K. Funabiki, M. Matsui, H. Miura, H. Yanagi, Advanced Functional Materials 19 (2009) 17–43.
[11] X.O. Yin, X.Z. Liu, L. Wang, B. Liu, Electrochemistry Communications 12 (2010) 1241–1244.
[12] M. Durr, A. Schmid, M. Obermaier, S. Rosselli, A. Yasuda, G. Nelles, Natural Materials 4 (2005) 607–611.
[13] D.S. Zhang, T. Yoshida, K. Furuta, H. Minoura, Journal of Photochemistry and Photobiology A: Chemistry 164 (2004) 159–166.
[14] S. Uchida, M. Timiha, H. Takizawa, M. Kawaraya, Journal of Photochemistry and Photobiology A: Chemistry 164 (2004) 93–96.
[15] T.N. Murakami, Y. Kijitori, N. Kawashima, T. Miyasaka, Chemistry Letters 32 (2003) 1076–1077.
[16] Y. Kijitori, M. Ikegami, T. Miyasaka, Chemistry Letters 36 (2007) 190–191.
[17] T. Yamaguchi, N. Tobe, D. Matsumoto, H. Arakawa, Chemical Communications (2007) 4767–4769.
[18] H. Lindstrom, A. Holmberg, E. Magnusson, S.E. Lindquist, L. Malmqvist, A. Hagfeldt, Nano Letters 1 (2001) 97–100.
[19] H. Lindstrom, A. Holmberg, E. Magnusson, L. Malmqvist, A. Hagfeldt, Journal of Photochemistry and Photobiology A: Chemistry 145 (2001) 107–112.
[20] G. Boschloo, J. Lindstrom, E. Magnusson, A. Holmberg, A. Hagfeldt, Journal of Photochemistry and Photobiology A: Chemistry 148 (2002) 11–15.
[21] X.Z. Liu, Y.H. Luo, H. Li, Y.Z. Fan, Z.X. Yu, Y. Lin, L.Q. Chen, Q.B. Meng, Chemical Communications (2007) 2847–2849.
[22] J. van de Lagemaat, K.D. Benkstein, A.J. Frank, Journal of Physical Chemistry B 105 (2001) 12433–12436.